Immunity

Supplemental Information

Cytomegalovirus Infection Drives Adaptive Epigenetic Diversification of NK Cells with Altered Signaling and Effector Function

Heinrich Schlums, Frank Cichocki, Bianca Tesi, Jakob Theorell, Vivien Beziat, Tim D. Holmes, Hongya Han, Samuel C.C. Chiang, Bree Foley, Kristin Mattsson, Stella Larsson, Marie Schaffer, Karl-Johan Malmberg, Hans-Gustaf Ljunggren, Jeffrey S. Miller, and Yenan T. Bryceson

SUPPLEMENTAL INFORMATION

Schlums, Cichocki *et al.*

SUPPLEMENTAL EXPERIMENTAL PROCEDURES

Antibodies

For flow cytometry, fluorochrome-conjugated antibodies to the surface epitopes CD3 (S4.1, Invitrogen; OKT3, Biolegend or SK7, BD Biosciences), CD4 (S3.5, Invitrogen), CD8 (3B5, Invitrogen), CD14 (M5E2, BD Biosciences), CD19 (HIB19, BD Biosciences), CD45RA (MEM-56, Invitrogen), CD56 (NCAM16.2, BD Biosciences or HCD56, Biolegend), CD57 (HCD57, Biolegend or NK-1, BD Biosciences), CD85j (GHI/75, Biolegend), CD107a (H4A3, BD Bioscience), NKG2A (Z199, Beckman Coulter), NKG2C (134591, R&D Systems or REA205, Miltenyi Biotec), NKp30 (p30-15, BD Biosciences), KIR2DL1/DS1 (EB6, Beckman Coulter), KIR2DL2/DS2/DL3 (GL183, Beckman Coulter), KIR2DS4 (179315, R&D Systems), KIR3DL1 (DX9, Biolegend), and KIR3DL2 (DX31, Biolegend; custom conjugation) were used. Intracellular staining of cytokines was performed using fluorochrome-conjugated antibodies to TNF (6401.11, BD Biosciences) and IFN-γ (B27, BD Biosciences). Intracellular signaling molecules and transcription factors were stained with fluorochrome-conjugated antibodies to FcεRγ (polyclonal Ab, Upstate), CD3ζ (6B10.2, Biolegend, eBioscience or Santa Cruz), SYK (4D10, BD Biosciences), ZAP-70 (1E7.2, BD Biosciences), phospho-p38 MAPK (36/p38 [pT180/pY182]; BD Biosciences), phospho-NF-κB p65 (K10-895.12.50; BD Biosciences), T-bet (O4-46, BD Biosciences), Eomes (WD1928, eBioscience), PLZF (Mags.21F7, eBioscience), and Helios (22F6,

Biolegend). The antibody for intracellular staining of SAP (1C9, Abnova) was conjugated to Alexa Fluor 488 or 647 (Invitrogen). Intracellular EAT-2 was stained using a rabbit polyclonal antibody (Proteintech Group) followed by secondary staining with fluorochrome conjugated anti-rabbit reagents (Invitrogen). For secondary surface stainings, fluorochrome-labeled anti-mouse IgM (Biolegend or eBioscience) and Streptavidin (Biolegend or Invitrogen) were used.

Bisulfite sequencing

For bisulfite sequencing of the *SH2D1B* promoter, the following forward and reverse primers were used for PCR: 5'-TTGGGGGTGAATTTTAGGTTAAT-3' and 5'-CACAAAAACACAAAACTCCTAATATC-3'. For bisulfite sequencing of the *FCER1G* promoter, the following forward and reverse primers were used for PCR: 5'-GTGGTGGTGTATGTTTGTAATGTTAGT-3' and 5'-CCTAACCCACAAAATAAAAAAACTTT-3'. For bisulfite sequencing of the *ZBTB16* intron 1 region, the following forward and reverse primers were used for PCR: 5'-AAGTGATATTTTGAAGTTGGTTTGT-3' and 5'-TTAAAACCCTTATCTCCCCATAC-3'. Primers were designed using the MethPrimer program (Li and Dahiya, 2002). PCR products were cloned into the TOPO-XL vector (Invitrogen) and sequenced.

Bisulfite sequencing genome-wide methylation analyses

For genome-wide methylation analysis, bisulfite-converted DNA was analyzed using the Infinium HumanMethylation450 BeadChip platform (Illumina). From each 450K array, a data report was generated using GenomeStudio

(Illumina). An initial filter was applied to the data by removing all probes previously described as cross-reactive (n=29230), as well as probes targeting polymorphic CpGs with an allele frequency in the European population higher than 30% (n=1969) (Chen et al., 2013). The output files were thereafter imported into the Bioconductor package *lumi* within R version 2.15.3 (Du et al., 2008). In total, 65 probes targeting SNPs, 10699 probes mapping to sex chromosomes, and 7170 probes with a detection p-value > 0.01 in more than 95% of the samples were removed. Quality control plots at this stage revealed an outlier sample that was removed from the analysis. The outlier was likely explained by too low input DNA for the array hybridization. A total of 436,444 methylation probes were subjected to color adjustment and quantile normalization within *lumi*, followed by correction for probe design using the Beta Mixture Quantile dilation algorithm, as previously described (Marabita et al., 2013). The *lumi* package was also used for generation of quality control plots and for multidimensional scaling analysis. Pairwise comparison plots and correlation plots were made using R version 2.15.3.

The normalized dataset was imported into the Bioconductor package *ChAMP*, within R version 3.0.2 (Morris et al., 2014). M-values, obtained from a log2 ratio of methylated probe intensity and unmethylated probe intensities, were used for the statistical analyses. The following pairwise comparison were performed: Early mature $CD56^{dim}CD57^{-}$ NK cells versus adaptive $CD56^{dim}CD57^{bright}EAT\text{-}2^{-}$ NK cells as well as effector $CD8^{+}$ T cells versus adaptive $CD56^{dim}CD57^{bright}EAT\text{-}2^{-}$ NK cells. The package *limma* was used to call single differentially methylated probes between these cell subsets. Only probes with an adjusted p-value < 0.05 (Benjamini-Hochberg method) were

considered differentially methylated. The Probe Lasso DMR Hunter implemented in *ChAMP* was used to identify differentially methylated probe regions. The parameters were set so that a minimum of 3 probes were necessary to call a DMR, and 3,000 bp was set for the maximum lasso size. An adjusted p-value of 0.05 was set as cut-off for calling DMRs. Further analysis were performed in R version 3.0.2. Upon publication, DNA methylation data will be available in publicly accessible repositories. In order to correlate gene expression with DMR, an average β-value change in methylation was calculated for each DMR involving a differentially expressed gene. The analysis was performed using R version 3.0.2.

Chromatin immunoprecipitations

Primary human peripheral blood NK cells from healthy donors were cross-linked with 1% formaldehyde and sheared with a Misonix sonicator. For each sample, 1×10^6 cell equivalents of chromatin were immunoprecipitated with the EZ-ChIP chromatin immunoprecipitation kit (Millipore) using 1 µg each of the following ChIP-grade antibodies: IgG isotype (Millipore), RNA polymerase II (CTD4H8, Millipore) and PLZF (2A9, Active Motif). Cross-links were reversed by incubation at 65°C with the addition of proteinase K overnight. Enrichment of RNA pol II and PLZF binding to promoter regions was determined by qRT-PCR using SYBR green reagents (QIAGEN) on a 7500 real-time PCR system (Applied Biosystems). Primer sequences for *FCER1G* were forward 5'-AAGAGCCCAGATCTCCCAAC-3' and reverse 5'-GCTGGAATCATCTTGGGCTG-3', for *SH2D1B* forward: 5'-ATTGCCTCCCTAGCCATGAG-3' and reverse: 5'-

GCTACCTCTTCCTCTAGCGG-3', for *SYK* forward 5'-ACTAGTGCGCCGTGAAGTCT-3' and reverse 5'-GGCCCTTTCCTTTTGCTATG-3', for *CD247* forward 5'-CTCAAACCTCCAGGGCTTC-3' and reverse 5'-GGGACGGTTAGGAGAAAAGG-3', for *SH2D1A* forward 5'-TGGGTCCACATACCAACAGA-3' and reverse: 5'-AACACACACCCTTGCACTCA-3', ZAP70 forward 5'-GCCTGTGATTTTCCTTGAGC-3' and reverse: 5'-GCAAGCAGGCTTGTCTGAA.-3'.

Multidimensional flow cytometry analysis using Barnes-Hut t-distributed stochastic neighbor embedding

Novel methods based on t-distributed stochastic neighbor embedding (t-SNE), including ViSNE and ACCENSE (Amir el et al., 2013; Shekhar et al., 2014), have proven useful in truthfully representing multidimensional flow cytometry data. For large datasets, however, conventional t-SNE implementations are limited, as the computational time increases exponentially with the number of variables examined. This has led to the development of Barnes-Hut t-SNE that uses vantage-point trees to compute sparse pairwise similarities between the input data objects based on a variant of the Barnes-Hut algorithm, to approximate the forces between the corresponding points in the embedding (according to Laurens van der Maaten, http://arxiv.org/abs/1301.3342).

The raw flow cytometry data was imported into FlowJo (v9.7.5, Tree Star) and compensated. Lymphocytes were gated on forward scatter and side scatter characteristics, single cells on forward scatter height versus forward

scatter area, followed by a gate on live, $CD3^-$, $CD14^-$, and $CD19^-$ cells. This resulted in a population that was further gated on $CD56^+$ and/or $CD57^+$ cells to define NK cells. Subsequently, data from 10,000 gated NK cells were concatenated, and a linearized interpretation of the data (channel numbers) was exported as comma separated values. The data was then preprocessed using R (version 3.15.3, 64 bit). First, the nine parameters CD56, CD16, CD57, CD7, CD161, NKG2A, NKG2C, FcεRγ, EAT-2, and SYK (Figure 7H-J) or CD56, CD16, CD57, NKG2A, NKG2C, Eomes, FcεRγ, Helios, PLZF and T-bet (Figure S7B-D), respectively, were selected and normalized according to the formula 100*((x-(min col(x)))/(max xol(x))-(min col(x))), where x is the value, and max/min col(x) represent the highest and the lowest values in the parameter where x is present. These data subsets, containing nine and ten parameters respectively, were converted to a binary .dat format using a python script (kindly written by Marcus Holm, UPPMAX, Uppsala University, Sweden). Then, Barnes-Hut t-SNE was conducted (code written in C++, compiled on OS.X v10.9.2, available from http://homepage.tudelft.nl/19j49/t-SNE.html). The resulting binary .dat files were reconverted to .csv using python script (provided by Marcus Holm and available upon request). Graphics were produced using R and packages gplots, ggplot2, and RColorBrewer. Before graphing, the most positive and negative per mille of the data was reduced to their less extreme border so that normalization would spread the data representatively.

Functional and phospho-signaling flow cytometry assays

For assessment of functional responses, PBMC were resuspended in complete medium containing GolgiPlug and GolgiStop (both BD Biosciences) and incubated alone or mixed at a 2:1 ratio with target cells. For cytokine stimulation, PBMC were stimulated with 10 ng/ml IL-12 (Peprotech), 100 ng/ml IL-15 (Peprotech), and 100 ng/ml IL-18 (MBL) for 18 hours, followed by addition of GolgiPlug and culture for an additional 6 hours. Stimulation with 100 ng/ml PMA and 0.5 µM ionomycin (both Calbiochem) was performed for 6 hours. Insect cells were coated with rabbit IgG using serum from immunized rabbits (gift of Dr. E. Long, National Institutes of Health, Rockville, MD) and co-cultured with PBMC for 6h. For assessment of activation thresholds, increasing concentrations of rabbit serum during insect cell coating and PP2 (Calbiochem) in medium were used. Following stimulation, the cells were stained for flow cytometric analysis.

For assessing signaling protein phosphorylation downstream of IL-18 stimulation, freshly isolated PBMCs from selected healthy donors with a sizable population of FcεRγ$^-$ NK cells were rested overnight in RPMI complete. The next day cells were washed, resuspended at 10×10^6 cells/ml in RPMI complete and stimulated for 10 minutes with 100 ng/ml recombinant human IL-18 or left untreated at 37°C. Cells were immediately fixed at 37°C by addition of an equal volume of 4% formaldehyde in PBS. The cells were transferred to an equal volume of cold FACS buffer supplemented with 0.02% Triton X-100 and permeabilized on ice. Cells were washed, resuspended in PBS and fluorescently barcoded with or without 0.1 µg/ml Alexa Fluor 488-NHS ester (Invitrogen) at room temperature. After washing with FACS buffer the differently treated cells were pooled, resuspended in ice-cold 90%

methanol and kept at –20°C. Afterwards, cells were washed with FACS buffer, stained with unconjugated rabbit anti-FcεRγ followed by fluorochrome-conjugated anti-rabbit, lineage and phospho-specific antibodies at room temperature in FACS buffer containing 2% bovine serum albumin (BSA; Sigma-Aldrich). Cells were washed and resuspended in FACS buffer before acquisition on the flow cytometer.

To assess NK cell responses to autologous T cells, negatively isolated $CD4^+$ and $CD8^+$ T cells (Milteny Biotec) were labeled (CellTrace Violet, Invitrogen) and rested or activated in complete medium with human T-activator CD3/CD28 Dynabeads (Invitrogen) at a 1:1 ratio. After 60 hours, the cells were resuspended in complete medium containing GolgiPlug and GolgiStop and mixed with resting, purified autologous NK cells at a 4:1 ratio. Additionally, NK cells were mixed with P815 target cells and anti-human CD16 mAb at a 2:1 ratio. Co-cultures were incubated for 6 hours, stained and analyzed by flow cytometry.

Quantitative PCR

Donors were preselected for correlation between $NKG2C^+$ and FcεRγ /EAT-2 down-regulation. Adaptive ($CD3^-CD56^{dim}CD57^+NKG2C^+$) and conventional $CD57^+$ NK cells ($CD3^-CD56^{dim}CD57^+NKG2C^-$) were sorted on a BD FACS Aria III into RLT buffer (Qiagen). RNA was purified with an on-column DNase digestion (RNeasy, Qiagen). First-strand synthesis used Superscript II with random hexamers (Invitrogen). Real-time PCR analysis was performed using the $\Delta\Delta C_T$ method with an annealing temperature of 60°C. Primer sequences for *IL18R1* were forward 5'-CTTTGGTCCAAGAAGAACCG-3' and reverse 5'-

GAAGAACGCCGAGTTTGAAG-3', for *IL18RAP* were forward 5'-ATCCACTACGATTCGGTTGC-3' and reverse 5'-CAGTCTCAGCTGCCAAAGTG-3', for *IL12RB1* were forward 5'-TGAGTCTGCATCCGGATATG-3', rev: 5'-TCCTCTTCCTCTTCCTGCTG-3'), for *IL12RB2* were forward 5'-AGAATGTTGTCCATGCCCTC-3' and reverse 5'-CAGTTCTCTGCCCACTCGTA-3', and for RNA 18s were forward 5'-GTAACCCGTTGAACCCCATT-3' and reverse 5'-CCATCCAATCGGTAGTAGCG-3'.

Western blots

Adaptive and conventional NK cells were sorted by flow cytometry as $CD3^-CD56^{dim}CD57^+NKG2C^+NKp30^-$ and $CD3^-CD56^{dim}CD57^+NKG2C^-NKp30^+$ respectively. Cells were subsequently stimulated with 100 ng/ml of IL-12 for 30 minutes and lysed in RIPA buffer containing phosStop phosphatase inhibitor cocktail and protease inhibitors (both Roche). Membranes were probed for phospho-STAT4 (Y693) and GAPDH (both Cell Signaling Technologies).

In vitro proliferation assays with CMV-infected monocyte co-culture

$CD3^-CD56^+$ NK cells and $CD14^+$ monocytes were isolated from the peripheral blood of CMV seropositive healthy donors by magnetic bead selection (StemCell Technologies). Monocytes were either mock-infected or infected with the TB40/E clinical CMV strain (Riegler et al., 2000), which was modified to include a GFP reporter, at a multiplicity of infection of 0.05. Thereafter, monocytes were mixed at a 1:1 ratio with autologous proliferation dye-labeled

NK cells (CellTrace, Invitrogen) and cultured in RPMI medium (Gibco) supplemented with 10% fetal bovine serum plus 10 ng/ml IL-15 (NIH) for 10 days. After 2 days of culture, hyper anti-CMV IgG (Cytogam, CSL Behring) at a concentration of 1:100 was added to some cultures. CMV infection of monocytes was confirmed by fluorescent microscopy 5 days post-infection. Following co-cultures, NK cells were stained with flurorescently-conjugated antibodies and analyzed by flow cytometry. The frequencies and proliferation of NK cell subsets was determined using FlowJo (v9.8.2).

REFERENCES

Amir el, A.D., Davis, K.L., Tadmor, M.D., Simonds, E.F., Levine, J.H., Bendall, S.C., Shenfeld, D.K., Krishnaswamy, S., Nolan, G.P., and Pe'er, D. (2013). viSNE enables visualization of high dimensional single-cell data and reveals phenotypic heterogeneity of leukemia. Nat Biotechnol *31*, 545-552.

Chen, Y.A., Lemire, M., Choufani, S., Butcher, D.T., Grafodatskaya, D., Zanke, B.W., Gallinger, S., Hudson, T.J., and Weksberg, R. (2013). Discovery of cross-reactive probes and polymorphic CpGs in the Illumina Infinium HumanMethylation450 microarray. Epigenetics *8*, 203-209.

Du, P., Kibbe, W.A., and Lin, S.M. (2008). lumi: a pipeline for processing Illumina microarray. Bioinformatics *24*, 1547-1548.

Hwang, I., Zhang, T., Scott, J.M., Kim, A.R., Lee, T., Kakarla, T., Kim, A., Sunwoo, J.B., and Kim, S. (2012). Identification of human NK cells that are deficient for signaling adaptor FcRgamma and specialized for antibody-dependent immune functions. Int Immunol.

Li, L.C., and Dahiya, R. (2002). MethPrimer: designing primers for methylation PCRs. Bioinformatics *18*, 1427-1431.

Marabita, F., Almgren, M., Lindholm, M.E., Ruhrmann, S., Fagerstrom-Billai, F., Jagodic, M., Sundberg, C.J., Ekstrom, T.J., Teschendorff, A.E., Tegner, J., and Gomez-Cabrero, D. (2013). An evaluation of analysis pipelines for DNA methylation profiling using the Illumina HumanMethylation450 BeadChip platform. Epigenetics *8*, 333-346.

Morris, T.J., Butcher, L.M., Feber, A., Teschendorff, A.E., Chakravarthy, A.R., Wojdacz, T.K., and Beck, S. (2014). ChAMP: 450k Chip Analysis Methylation Pipeline. Bioinformatics *30*, 428-430.

Shekhar, K., Brodin, P., Davis, M.M., and Chakraborty, A.K. (2014). Automatic Classification of Cellular Expression by Nonlinear Stochastic Embedding (ACCENSE). Proc Natl Acad Sci U S A 111, 202-207.

SUPPLEMENTAL FIGURES

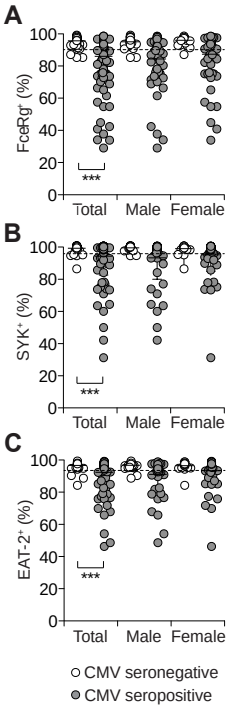

Figure S1, related to Figure 1. FcεRγ^{-}, SYK^{-}, and EAT-2^{-} adaptive NK cell phenotypes are not associated with gender

PBMC from healthy human blood donors were surface stained with antibodies to lineage and differentiation markers, and subsequently stained intracellularly with antibodies to signaling proteins, as indicated. Graphs depict the frequency of CD3^{-} CD56^{dim} NK cells expressing FcεRγ, SYK, and EAT-2 plotted versus sex of the individuals. Each circle represents one individual. Empty circles denote CMV seronegative individuals, whereas filled circles denote CMV seropositive individuals. Dotted lines indicate a threshold for outliers calculated as the mean of CMV seronegative individuals added 3 SD. *** $P < 0.001$ (unpaired, two-tailed, Mann-Whitney test).

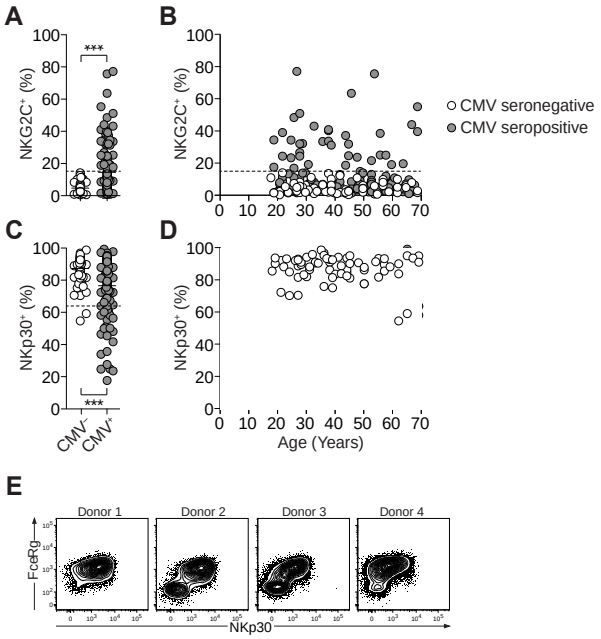

Figure S2, related to Figure 2. NKG2C and NKp30 expression is correlated with cytomegalovirus seropositivity

PBMC from healthy human blood donors were surface stained with antibodies to lineage and differentiation markers and subsequently stained intracellularly with antibodies to signaling proteins as indicated. (A-D) Graphs depict the frequency of $CD3^{-}CD56^{dim}$ NK cells expressing NKG2C and NKp30 from 196 healthy blood donors. Additionally, the frequency of $CD3^{-}CD56^{dim}$ NK cells expressing NKG2C and NKp30 are plotted versus age of the individuals. Each circle represents one individual. Empty circles denote CMV seronegative individuals, whereas filled circles denote CMV seropositive individuals. Dotted lines indicate a threshold for outliers calculated as the mean of CMV seronegative individuals plus 1 SD. *** $P < 0.001$ (unpaired, two-tailed, Mann-Whitney test). (E) Contour plots depict FcεRγ versus NKp30 expression in $CD3^{-}CD56^{dim}$ NK cells from 1 representative CMV seronegative donor (donor 1) and 3 representative CMV seropositive donors (donor 2-4) with FcεRγ deficiency. This is consistent with what has previously been shown by Kim and colleagues (Hwang et al., 2012).

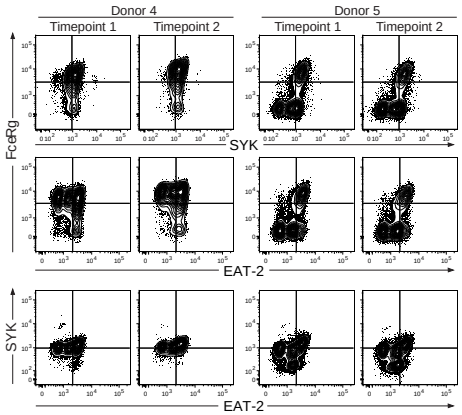

Figure S3, related to Figure 3. Stable patterns of signaling protein expression in NK cells from CMV seropositive individuals

PMBC from healthy human blood donors were surface stained with antibodies to lineage and differentiation markers, and subsequently stained intracellularly with antibodies to signaling proteins, as indicated. Contour plots depict respective signaling protein expression, as indicated, in $CD3^{-}CD56^{dim}$ NK cells from 2 representative adult CMV seropositive donors lacking signaling proteins. The time points are 28 (donor 4) and 33 (donor 5) months apart.

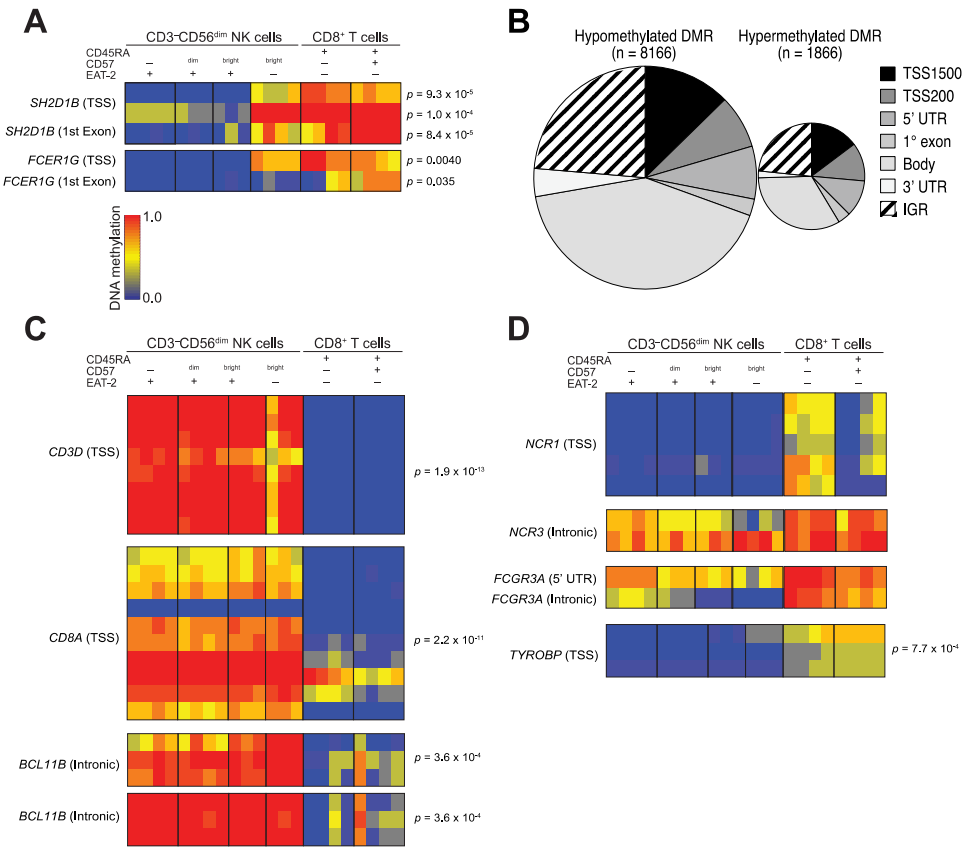

Figure S4, related to Figure 4. DNA methylation in NK cell subsets
Early mature $CD3^{-}CD56^{dim}CD57^{-}$, late mature $CD3^{-}CD56^{dim}CD57^{bright}EAT\text{-}2^{+}$, and adaptive $CD3^{-}CD56^{dim}CD57^{bright}EAT\text{-}2^{-}$ NK cells, as well as naïve $CD3^{+}CD8^{+}CD45RA^{+}CD57^{-}$ and effector $CD3^{+}CD8^{+}CD45RA^{+}CD57^{bright}$ T cell subsets, were sorted from 4 CMV seropositive donors. Genomic DNA from each subset was treated with sodium bisulfite and subjected to genome-wide DNA methylation profiling. (A) Heat maps represent the DNA methylation for a set of differentially regulated *SH2D1B and FCER1G* probes. (B) Pie-charts depict the gene distribution of hypomethylated and hypermethylated DMRs, respectively. (C) Heat maps represent the DNA methylation in DMRs for T cell-specific genes *CD3D*, *CD8A*, and *BCL11B*. (D) Heat maps represent the DNA methylation in probes and DMRs for more NK cell-restricted genes: *NCR1* (encoding NKp46), *NCR3* (encoding NKp30), *FCGR3A* (encoding CD16), and *TYROBP* (encoding DAP12). A β-value close to zero corresponds with no methylation, and a β-value close to 1 corresponds with full methylation of the probed region.

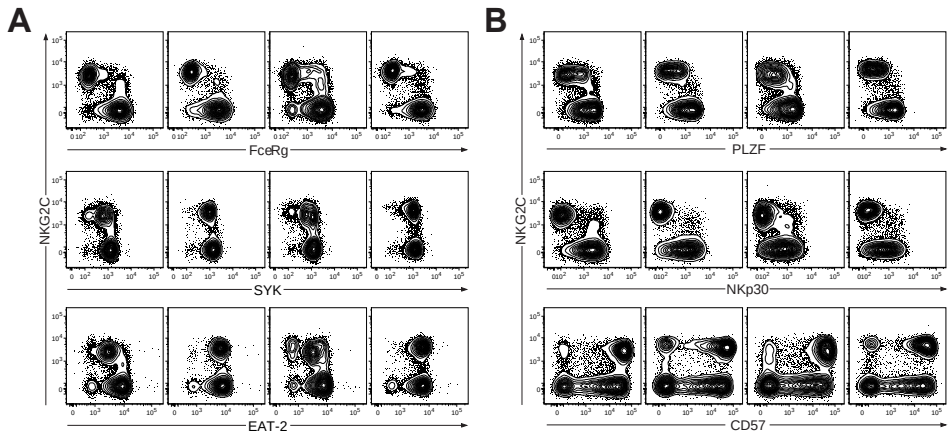

Figure S5, related to Figure 5. Phenotypic characteristics of donors used for gene expression analyses

(A,B) PMBC from healthy human blood donors were surface stained with antibodies to lineage and differentiation markers, and subsequently stained intracellularly with antibodies to signaling proteins and PLZF, as indicated. (E) Contour plots depict NKG2C versus signaling protein expression, as indicated, in $CD3^{-}CD56^{dim}$ NK cells. (F) Contour plots depict NKG2C versus PLZF, NKp30, or CD57 expression, as indicated, in $CD3^{-}CD56^{dim}$ NK cells. For microarray analyses, gene expression was evaluated in sorted $CD3^{-}CD56^{dim}CD57^{bright}NKG2C^{-}$ and $CD3^{-}CD56^{dim}CD57^{bright}NKG2C^{+}$ (corresponding to $Fc\varepsilon R\gamma^{dim/-}$) NK cell subsets from these 4 donors.

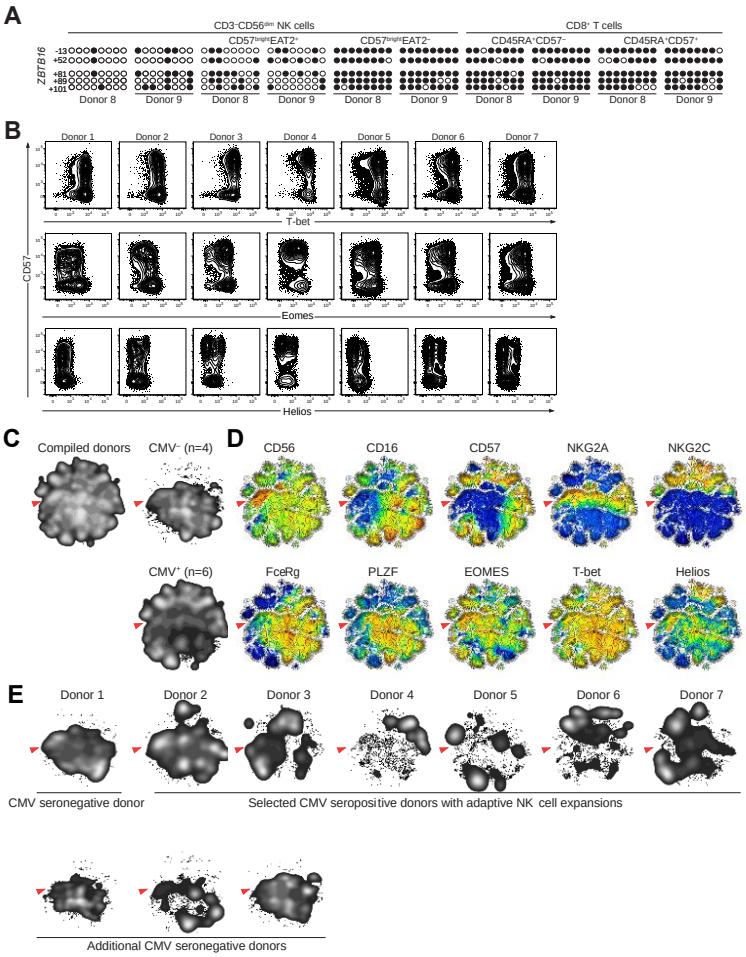

Figure S6, related to Figure 6. Hypermethylation of *ZBTB16* intronic regulatory region in adaptive NK cells and expression of transcription factors T-bet, EOMES, and Helios in NK cell subsets

(A) Early mature $CD3^{-}CD56^{dim}CD57^{-}$, late mature $CD3^{-}CD56^{dim}CD57^{bright}EAT\text{-}2^{+}$ and adaptive $CD3^{-}CD56^{dim}CD57^{bright}EAT\text{-}2^{-}$ NK cells, as well as naïve $CD3^{+}CD8^{+}CD45RA^{+}CD57^{-}$ and effector $CD3^{+}CD8^{+}CD45RA^{+}CD57^{bright}$ T cell subsets, were sorted from 2 CMV seropositive donors. Genomic DNA from each cell subset was treated with sodium bisulfite, purified and amplified by PCR using primers specific for the intronic regulatory region of *ZBTB16*. PCR fragments were cloned, sequenced and analyzed for CpG methylation content. Each row represents one sequenced PCR clone. Open circles represent unmethylated cytosines, and closed circles represent methylated cytosines.

(B-E) PBMC from healthy human blood donors were surface stained with antibodies to lineage and differentiation markers and subsequently stained intracellularly with antibodies to FcεRγ, PLZF, T-bet, EOMES, and Helios. (B) Contour plots depict CD57 expression versus expression of T-bet, EOMES, or Helios in $CD3^{-}CD56^{dim}$ NK cells from 1 representative CMV seronegative donor (donor 1) and 6 CMV seropositive donors with signaling protein deficiencies. (C-E) Barnes-Hut t-distributed stochastic neighbor embedding (t-SNE) analysis of 10-parametric data was performed on $CD3^{-}CD56^{+}$ NK cells from 4 CMV seronegative and six selected CMV seropositive donors (donors 2-7). (C) Event density in the t-SNE field for all donors compiled together or CMV seronegative and CMV seropositive donors compiled separately. (D) Expression levels for single parameters in t-SNE field, as indicated. Red represents high expression, whereas blue represents low expression. (E) Event density in the t-SNE field for $CD3^{-}CD56^{+}$ NK cells from individual donors, as indicated. Red arrows indicate the $CD56^{bright}$ NK cell population.

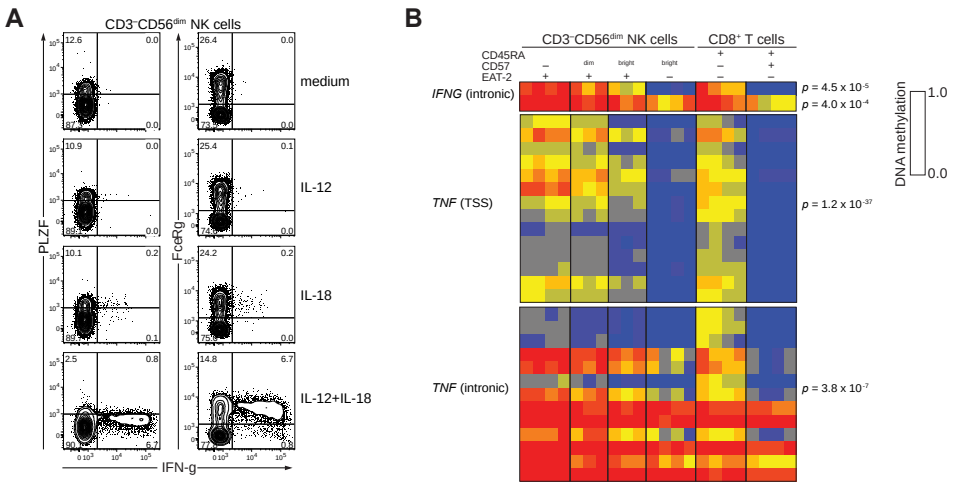

Figure S7, related to Figure 7. IFN-γ responses and hypomethylation of the *IFNG* and *TNF* regulatory regions in adaptive NK cells.

(A) PBMC from CMV^{+} individuals with a clear correlation between PLZF and FcεRγ expression were left untreated or stimulated for 24 hours with combinations of IL-12 and IL-18, then stained for intracellular PLZF, FcεRγ, and IFN-γ followed by analysis by flow cytometry. Plots show IFN-γ expression versus PLZF or FcεRγ in gated CD3^{-} CD56^{dim} NK cell subsets.

(B) Heat maps show the DNA methylation in different cell subsets for a set of differentially regulated *IFNG* probes and *TNF* probes within two DMRs, as indicated. A β-value close to zero corresponds with no methylation, and a β-value close to 1 corresponds with full methylation of the probed region.